J Incl Phenom Macrocycl Chem (2007) 59:167–176
DOI 10.1007/s10847-007-9309-0

ORIGINAL ARTICLE

Experimental and theoretical spectral properties of ethyl 2-(7-hydroxy-2-oxo-2H-chromen-4-yl)acetate doped sol-gel materials: new materials with potential optical application

G. Ahmed · B. Koleva · S. Gutzov · I. Petkov

Received: 10 November 2006 / Accepted: 6 March 2007 / Published online: 12 April 2007

Abstract Silica xerogels and monoliths, containing ethyl 2-(7-hydroxy-2-oxo-2H-chromen-4-yl)acetate (K4) or Sm^{3+} ions and K4 are prepared by sol-gel technique. NMR investigations, UV/Vis, IR- and luminescence spectral properties of K4 in solution and in monoliths are presented. The IR-spectroscopic properties of the prepared sol-gel materials are examined by applying the reduced-difference procedure to non-polarized IR-spectra. The results show that the sol-gel medium did not interact with K4 as well as in the presence of Sm^{3+} ions the K4 form a $[Sm(L)_2(H_2O)_4] \times (NO_3)_3$ complex in the matrix.

Keywords Coumarin · IR- and UV/Vis spectroscopy · Luminescence · Sm^{3+}-complex · Sol-gel

Electronic Supplementary Material The online version of this article (doi:10.1007/s10847-007-9309-0) contains supplementary material, which is available to authorized users.

G. Ahmed (✉) · I. Petkov
Department of Organic Chemistry, Organic Photochemistry Group, University of Sofia ''St Kliment Ohridski'', 1, James Bauchier Boulevard, 1164 Sofia, Bulgaria
e-mail: ohga@chem.uni-sofia.bg

B. Koleva
Department of Analytical Chemistry, University of Sofia ''St Kliment Ohridski'', 1, James Bauchier Boulevard, 1164 Sofia, Bulgaria

S. Gutzov
Department of Physical Chemistry, University of Sofia ''St Kliment Ohridski'', 1, James Bauchier Boulevard, 1164 Sofia, Bulgaria

Introduction

Nowadays, sol-gel process is used for the preparation of porous gel glasses doped with organic molecules at relatively low temperatures (< 150°C). As a result organic dyes retain their optical properties and are successfully incorporated into a rigid, inorganic amorphous host [1-4].

A new challenge of sol-gel technologies is the preparation of organic modified ceramics (ormocer) and hybrid optical materials containing optical active organic molecules and inorganic ions. Sol-gel derived inorganic networks doped with lanthanoid ions and organic compounds or organic complexes have demonstrated excellent optical properties: transparence, coloration and high-quantum efficiency [5].

Coumarins and their complexes with metal ions have been studied extensively in the past years. They are of interest because of their luminescence properties and biological activities. Some of the luminescent lanthanide complexes have application as planar waveguide amplifiers, plastic lasers or light-emitting diodes [6–8]. The physiological, anticoagulant, spasmolytic, bacteriostatic and antitumor activities of coumarins and their complexes are important for pharmacy and medicine [9,10].

In this paper, we describe the preparation and properties of new organic-inorganic hybrids that are investigated for optical applications. The UV/Vis, IR- and luminescence properties of ethyl 2-(7-hydroxy-2-oxo-2H-chromen-4-yl) acetate (K4) are investigated.

Experimental

Synthesis

This coumarin is synthesized according to the method of Dann and Illing [11], the Pechmann reaction of 1,3-di-

hydroxybenzene and the substituted β-keto-ester (diethyl-3-oxo-pentandioate in sulfuric acid gives ethyl (7-hydroxy-2-oxo-2H-chromen-4-yl)acetate [11,12].

The obtaining of the K4 is proved by showing the chemical shifts in ^{1}H NMR spectrum in DMSO-d_6, δ ppm, 10.610 (s, 1H, OH), 7.526–7.473 (m, 3H, Ar), 6.825 (s, 1H, 3-coum), 4.122 (m, 2H, OCH_2CH_3), 3.927 (s, 2H, CH_2), 1.125 (t, 3H, CH_3).

The preparation of the monoliths in this contribution is based on two preparation schemes described in [13], which were modified to obtain large, transparent monoliths for transmittance UV/Vis investigations. The acid-based hydrolysis is followed by gelation at pH = 6–7, so that gels can be formed reproducibly for up to 30 min.

Monoliths containing coumarins were prepared by the following sequence: TEOS (98%; Aldrich) and absolute EtOH (99.8%; Riedel-de Haën) are mixed together in a 1:1 molar ratio. For the Sm^{3+}-doped gels a 0.57 M solution of samarium nitrate with pH~3 was added to the mixture of TEOS and absolute EtOH before hydrolysis. After homogenization of the mixture distilled H_2O in a 1:4 molar ratio and 0.23 M HCl for the hydrolysis were added. This process takes place at pH~2 for 2 h.

Because coumarins are pH sensitive we had to alkaline the medium after HCl catalyzed hydrolysis up to pH = 6–7 before adding coumarin solution. A mixture of 0.14 M NH_3 and C_2H_5OH/H_2O in a 1:4 molar ratio was used to alkaline the solution. Gelation of monoliths takes place by pouring the sol into covered plastic Petri dishes. Petri dishes were covered for 24 h for gel aging. After aging the covers were removed and replaced by covers with three holes to allow slow solvent evaporation. The area of holes is about 1–2% from the cover area.

Monolithic, transparent xerogels without colorations were obtained. The described procedure allows to prepare reproducibly transparent, crack-free monoliths with radius r = 1.25–1.4 cm, thickness d = 0.2–0.3 cm and weight g = 1.8–1.9 g. The molar ratios K4/Si = 4.46×10^{-6} and Sm^{3+}/Si = 0.01. According to IR and TG investigations, such gels normally contain about 25% H_2O, including both OH^- groups and H_2O [12], where the water content is higher for gels, highly doped with rare-earth ions [14–16]. The gels are amorphous, proved by X-ray diffraction.

Materials and methods

UV/Vis spectra were recorded using a Thermo Spectronic ''Unicam UV 500'' UV/Vis spectrophotometer. The luminescence spectra were recorded with Varian ''Cary Eclipse'' fluorescence spectrophotometer. Both UV/Vis and luminescence spectra of xerogels were recorded directly on the monoliths. For the 1×10^{-4} M ethanol solutions of K4 quartz cuvettes were used.

Scanning electron microscope (SEM) investigations are performed on a standard JEOL 5510 microscope.

The ^{1}H NMR spectra are recorded on a Bruker 250 Spectrometer at 298 K.

The IR spectra were recorded on a Bomem-Michelson 100 FTIR-spectrometer. The conventional (non-polarized) solid IR spectra have been obtained using KBr disk technique. The position (ν_i) and corresponding integral absorbancies (A_i) for each i-peak were determined by deconvolution and subsequent curve-fitting procedure at 50:50% ratio of Lorentzian to Gaussian peak functions. The means of two treatments were compared by Student's t-test [17–19]. The experimental IR spectral curves have been acquired and processed by means of GRAMS/AI 7.01 IR spectroscopy (Thermo Galactic, USA) and STATISTICA for Windows 5.0 (StatSoft, Inc., Tulsa, OK, USA) program packages.

The method described in [20–24] for n-component systems consists in *subtraction* of two IR spectral curves, corresponding to samples, containing diverse concentrations of given structural units. The theory is listed in Supplementary material.

Quantum chemical calculations were performed by using DALTON 2.0 program package [25]. The output fails are visualized by means of ChemCraft program [26]. The geometry (K4) is optimized at two levels of theory: second-order Moller-Pleset perturbation theory (MP2) and density functional theory (DFT) using 6-311++G** basis set. DFT method employed is B3LYP, which combines Becke's three-parameter non-local exchange functional along with the correlation function of Lee, Yang and Parr [27,28]. Molecular geometry of the studied species was fully optimized by the force gradient method using Bernys' algorithm [29]. For every structure the stationary points found on the molecule potential energy hypersurfaces were characterized using standard analytical harmonic vibrational analysis. The absence of the imaginary frequencies, as well as of negative eigenvalues of the second-derivative matrix, confirmed that the stationary points correspond to minima of the potential energy hypersurfaces. The calculation of vibrational frequencies and IR intensities were checked for which kind of calculations performed agree best with the experimental data. The DFT method provide more accurate vibrational data, as far as the calculated standard deviations are 9 cm^{-1} (B3LYP) and 21 cm^{-1} (MP2), respectively. So, the B3LYP/6-311++G** data are presented for above discussed modes, where for the better correspondence between the experimental and theoretical values, a modification of the results using the empirical scaling factor 0.9614 [30] is made. Molecule orbital model of K4 is optimized starting with semi-empirical PM3 calculations and then refined at B3LYP/6-311++G** level of theory and basis set [31,32].

Results and discussion

Molecular geometry

According to the quantum chemical calculation, both by ab initio and DFT ones, two distinct stable conformers of K4 exist differing by internal rotation around the C-O bond in phenyl ring (Scheme 1): when C-C-O-H is equal to 0.2° and 179.6° (MP2/6-311++G**), respectively. When energies are corrected by zero point vibrational energy contribution, the first form is more stable with 2 kJ/mol. This conformer is characterized with absolutely flat aromatic conjugated system, where the maximal deviation of total planarity is less than 0.7°. The plane of carboxylic fragment is oriented near to perpendicular toward the plane of the benzene ring closing at an angle of 97.9°. The dipole moment in gas phase is 2.9873 Debay. The predicted geometry parameters of discussed form are summarized in Table 2 of Supplementary material, where due to the ab initio approach give the better structural parameters [27,28], the values are obtained by MP2/6-311++G**.

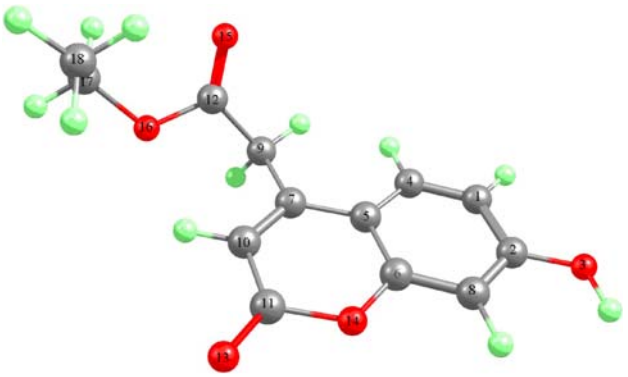

Scheme 1 Calculated geometry of K4 with E_{rel} of 0.4 kJ/mol at MP2/6-311++G** level of theory and basis set

Theoretical and experimental UV-spectral and luminescence data

All the investigated monoliths are transparent and colorless.

The violet color of the gels comes from transmitting excitation light. Figure 1 shows the high-optical quality transparence and strong, blue luminescence of the prepared samples. The SEM investigations confirm that the gels have a flat, crack-free surface (Fig. 2).

Absorption spectra of K4 in EtOH solution and in xerogel and gel co-doped with K4 and Sm^{3+} ions are presented in Fig. 3.

The spectrum of SiO_2-monolith without dopant is given for comparison. The spectra features can be explained with

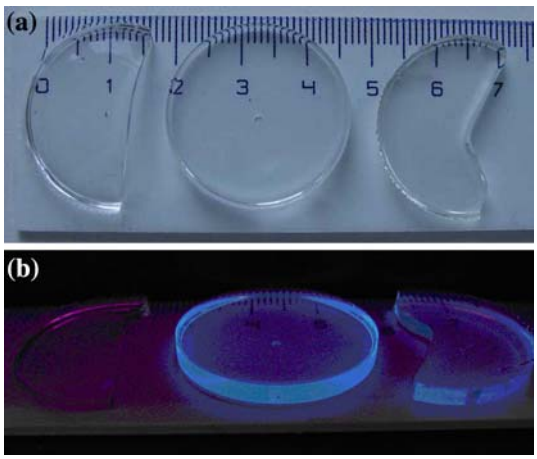

Fig. 1 Photograph of (from left to right) gel without modifying (G30); gel, modified with K4 (GK4); and gel, modified with K4 and Sm^{3+} ions (GK4Sm): **a** on ruler and **b** emission

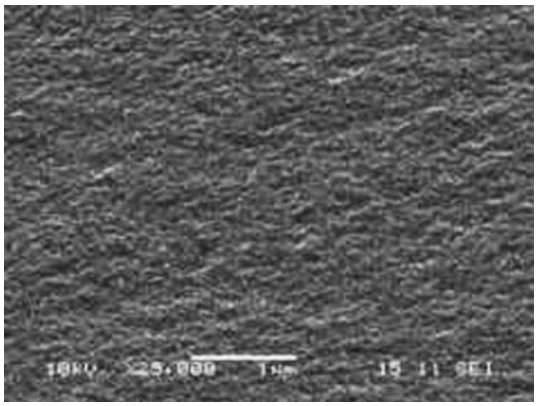

Fig. 2 Scanning electron microscope (SEM) results of the surface of a non-doped gel prepared (G30)

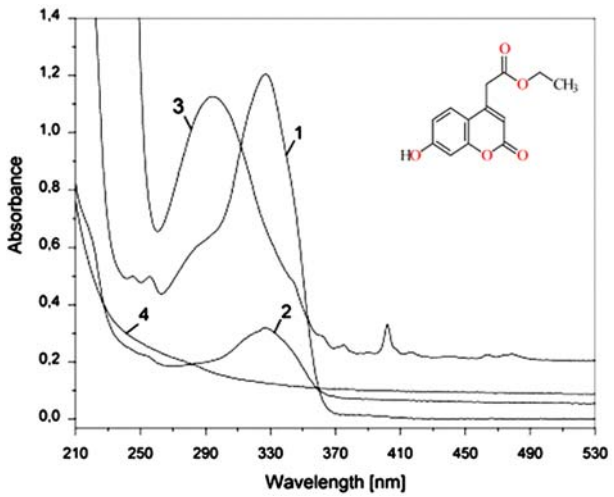

Fig. 3 UV/Vis spectra of (1) 1×10^{-4} M EtOH solution of K4; (2) GK4; (3) GK4Sm; and (4) G30

Table 1 UV procedure spectral patents by Gaussian analysis of K4 absorption spectra: x_c – peak position; A_{int} – integrated absorbance; ω –full half-width

No.	Transition	GK4 (d = 0.25 cm, r = 1.25 cm)		
		x_c (cm^{-1})	A_{int} (cm^{-1})	ω (cm^{-1})
1.	n → π^* (C=O)	29,038 ± 63	55 ± 10	1,062 ± 109
2.	n → π^* (C=O)	30,216 ± 103	25 ± 10	924 ± 183
3.	n → π^* (C=O)	30,636 ± 28	652 ± 11	2,859 ± 37
4.	n → π^* (C=O)	33,571 ± 100	189 ± 4	3,290 ± 92s
K4 solution (d = 1 cm)				
1.	n → π^* (C=O)	28,890 ± 22	478 ± 52	1,069 ± 21
2.	n → π^* (C=O)	30,019 ± 19	1,044 ± 184	1,467 ± 85
3.	n → π^* (C=O)	31,291 ± 89	1,451 ± 149	1,987 ± 69
4.	n → π^* (C=O)	33,571 ± 20	2,734 ± 19	5,195 ± 21
GK4Sm (d = 0.25 cm, r = 1.25 cm)				
1.	n → π^* (C=O)	29,461 ± 65	136 ± 18	1,497 ± 151
2.	CTT O^{2-} → Sm^{3+}	33,584 ± 17	3,751 ± 27	4,484 ± 41

well-known electronic transitions in organic molecules, which are given in Table 1.

A number of essential conclusions could be drawn with respect to the evolution of the spectra in solution and gel: (1) the method of ''basic'' gelation leads to the reproducible preparation of gels, transparent up to 230 nm; (2) the absorption spectrum of GK4Sm changes significantly in comparison to GK4, which is an indication for a complex formation; (3) the absorption maxima of K4 in solution and in gel is at 327 nm and the incorporation of Sm^{3+} leads to 60 nm change; and (4) there are significant differences in the full half-widths and relative absorption intensities after the doping of K4, suggesting an effective incorporation of the coumarin molecules in the silica gel network.

Gaussian analysis results from gels doped with K4 and Sm^{3+} are summarized in Table 1. The peak maxima x_c, integrated absorbance A and full half-width ω are presented.

Additional weak absorption peaks arising from Sm^{3+} f-f transitions at 27649 cm^{-1}, 26652 cm^{-1}, 24861 cm^{-1}, 23920 cm^{-1}, 21559 cm^{-1} and 20893 cm^{-1} also appear in the spectrum. The peaks due to f-f transitions are in agreement with theoretical expectations and measurements as published in [33]. The strong peak due to charge transfer transition (CTT) O^{2-} → Sm^{3+} is at 33584 !!cm^{-1}, the peak at 280 nm is in good agreement with measurements given in [34]. As a result of the Sm-doping the peak maxima in GK4Sm is blue shifted compared to the peak maxima of GK4.

Figure 4 represents the luminescence spectra of K4 in EtOH solution and in xerogel and gel co-doped with K4 and Sm^{3+}, which were measured at room temperature.

Table 2 Optimized geometry parameters of K4 at MP2/6-311++G** level of theory and basis set, using atom numbering scheme 2

Name definition	Bond lengths (Å)	Name definition	Angles (°)
R(1,2)	1.407	A(2,1,4)	120.0 (9)
R(1,4)	1.380	A(1,2,3)	116.8 (3)
R(2,3)	1.377	A(1,2,8)	119.5 (7)
R(2,8)	1.389	A(3,2,8)	123.5 (9)
R(4,5)	1.412	A(1,4,5)	121.5(0)
R(5,6)	1.412	A(4,5,6)	117.4 (6)
R(5,7)	1.451	A(4,5,7)	125.3 (7)
R(6,8)	1.394	A(6,5,7)	117.1 (6)
R(6,14)	1.372	A(5,6,8)	121.1 (3)
R(7,9)	1.530	A(5,6,14)	122.0 (8)
R(7,10)	1.358	A(8,6,14)	116.7 (7)
R(9,12)	1.521	A(5,7,9)	120.6 (7)
R(10,11)	1.445	A(5,7,10)	120.1 (0)
R(11,13)	1.219	A(9,7,10)	119.2 (0)
R(11,14)	1.440	A(2,8,6)	120.2 (2)
R(12,15)	1.224	A(7,9,12)	112.1 (3)
R(12,16)	1.383	A(7,10,11)	123.8 (1)
R(16,17)	1.494	A(10,11,13)	128.3 (4)
R(17,18)	1.528	A(10,11,14)	114.6 (2)
		A(13,11,14)	117.0 (3)
		A(9,12,15)	126.6 (3)
		A(9,12,16)	109.8 (2)
		A(15,12,16)	123.5 (4)
		A(6,14,11)	122.2 (0)
		A(12,16,17)	115.4 (4)
		A(16,17,18)	110.8 (5)
Dihedral angles (°)			
Name definition		Name definition	
D(4,1,2,3)	179.9	D(14,6,8,2)	179.9
D(4,1,2,8)	0.0	D(5,6,14,11)	0.1
D(2,1,4,5)	0.0	D(8,6,14,11)	179.9
D(1,2,8,6)	0.0	D(5,7,9,12)	130.4
D(3,2,8,6)	179.9	D(10,7,9,12)	50.9
D(1,4,5,6)	0.0	D(5,7,10,11)	0.0
D(1,4,5,7)	179.7	D(9,7,10,11)	178.5
D(4,5,6,8)	0.0	D(7,9,12,15)	102.3
D(4,5,6,14)	179.9	D(7,9,12,16)	77.9
D(7,5,6,8)	179.8	D(7,10,11,13)	179.9
D(7,5,6,14)	0.1	D(7,10,11,14)	0.1
D(4,5,7,9)	1.3	D(10,11,14,6)	0.0
D(4,5,7,10)	179.8	D(13,11,14,6)	179.9
D(6,5,7,9)	178.3	D(9,12,16,17)	179.0
D(6,5,7,10)	0.1	D(15,12,16,17)	1.1
D(5,6,8,2)	0.1	D(12,16,17,18)	77.6

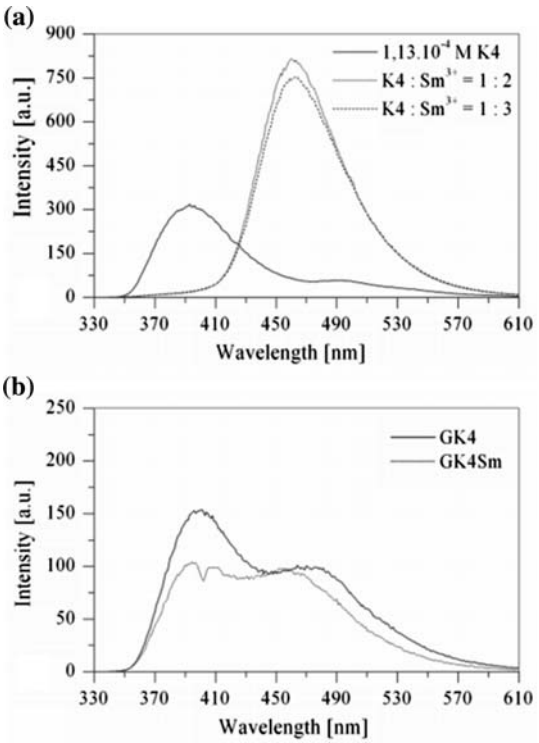

Fig. 4 Emission spectra: **a** 1.13×10^{-4} M EtOH solution of K4, solution K4/Sm^{3+} = 1:2 and solution K4/Sm^{3+} = 1:3; **b** GK4 and GK4Sm

All the samples are excited with λ_{ex} = 327 nm which corresponds to the absorption maxima of n → π* transition due to the C = O group in K4 molecules and have strong blue luminescence at 395 nm (25,316 cm^{-1}). The ethanol solution of K4 displays an additional peak at about 490 nm (20,408 cm^{-1}); the GK4 has luminescence maxima at 400 nm (25,000 cm^{-1}) and 480 nm (20,833 cm^{-1}), the GK4Sm at 395 nm (25,316 cm^{-1}) and 460 nm (21,739 cm^{-1}), and the solution K4/Sm^{3+} = 1:3 at 460 nm (21,739 cm^{-1}).

Our spectroscopic results in Table 1 give an indication that the incorporation into the gel network is a preferred way for coumarin incorporation into xerogels. According to [35] silica gels consist of SiO_4 tetrahedra, which are connected only by its corners and not by their edges of faces. The most probable sites of the large coumarin molecules in the silica network should be the free space between the SiO_4 tetrahedra.

The formation of coumarin complexes is important for the spectral properties of the investigated gels. Complex formation in systems containing coumarin and rare earth ions is discussed in [8,9].

Samarium-doped gels do not produce f-f luminescence at room temperature, which gives an indication that the Sm(III) ion is closely surrounded by H_2O molecules or OH groups, and do quench the rare earth luminescence [14–16,36]. The absence of luminescence of Ho(III) in silica gels is a well-known fact, but in contrast the same ion displays a strong luminescence at room temperature in oxide hosts [12,13].

According to the literature data, the Sm^{3+} complexes with coordination number 8, similar to $[Sm(L)_2 \times H_2O]^{3-}$, are characterized with the bands at luminescence spectrum, 346 nm and 468 nm [37]. This result assumed that the Sm^{3+} ion forms a complex with K4 with same coordination number. As far as the first band in our case is concerned, it is typical for pure compound embedded in the gel matrix, and the origin of the similar one in the spectrum of the GK4Sm system is due to K4. However, the band at 468 nm arises from the transitions from the emitting $^4G_{5/2}$ level to the ground ^6H_J levels. The broad band, which is not originated from Sm^{3+}, may be responsible for the intraligand emission. An energy transfer from the defects in the SiO_2 matrix to the Sm-K4 complex could be another possibility for improving the luminescence properties of hybrid materials based silica xerogels [14–16,36].

Theoretical and experimental IR-data

The important question about the interactions between K4 and gel, without modifying (G30) or Sm^{3+}–K4 interactions, which could be affected by the IR-spectroscopic and UV-properties of K4, requires a study on the IR-spectra of the pure K4 in solid state, in gel matrix and in the presence of the Sm^{3+} ions. The adequate examination of the influence of the medium on the peak position and integral absorbancies of IR-spectroscopic bands requires the knowledge of the origin of corresponding maximum in the IR-spectrum of compound studied as well as the influence of the intermolecular interactions on the IR-characteristic bands

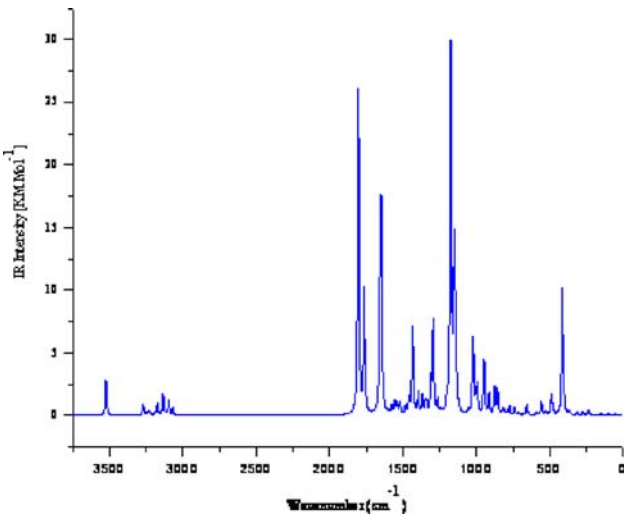

Fig. 5 Theoretical, predicted IR-spectrum of K4 at B3LYP/6-311++G** level of theory and basis set (non-scaled)

position in solid state. For this reason, a preliminary theoretical vibrational analysis could helpin the adequate assignment of each band to corresponding vibrational mode.

The theoretical IR-spectrum of K4 in gas phase is presented in Fig. 5. In both cases, a comparison between the calculated spectra and the experimental ones [Fig. 6A (1), (3)] in solid state is performed. The predicted IR-spectrum of K4 is characterized with the highest absorption maximum at 3389 cm^{-1} assigned to stretching mode of OH group (ν_{OH}). The bands at 3120–2945 cm^{-1} IR-region corresponds to in plane (i.p.) modes of benzene ring as well

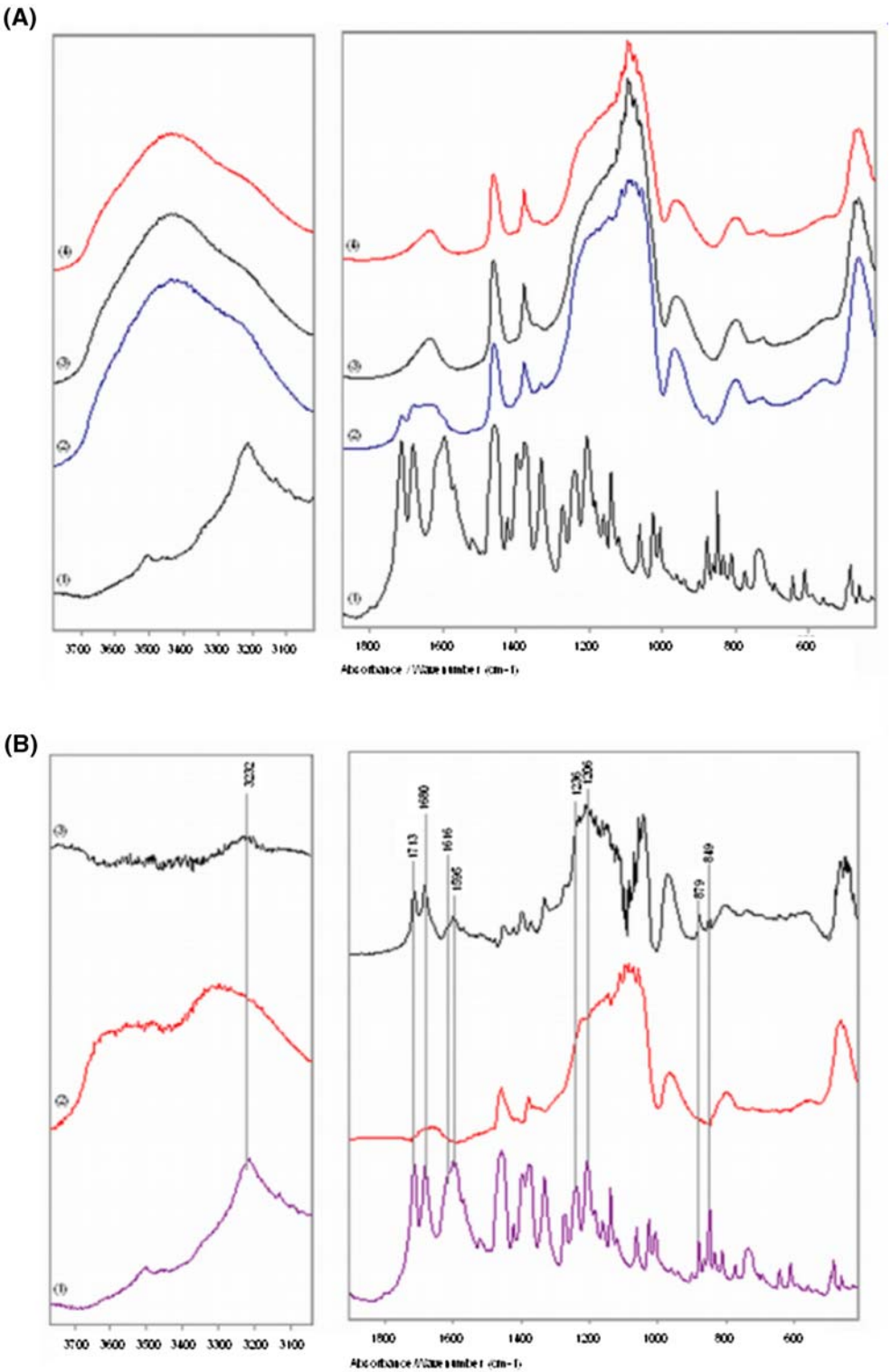

Fig. 6 A IR-spectra of K4 (1), Gel30 (2), GK4 (3) and GK4Sm (4). **B** Reduced IR-spectra: (1) K4 with subtracted solvent molecules (H_2O), which are not interacted; (2) G30 with subtracted solvent molecules (H_2O), which are not interacted; and (3) GK4 with subtracted solvent molecules (H_2O), which are not interacted, and G30 matrix bands

as of symmetric and asymmetric stretching CH_2 and CH_3 modes. The 1750–1500 cm^{-1} IR-spectroscopic region shows series of bands with mixed character starting with the 1735 cm^{-1} peak with predominant $\nu_{C=O}$ character of exocyclyc C=O band (Scheme 3 A in Supplementary material). The maximum at 1696 cm^{-1} assigned to $\nu_{C=O}$ of ester carbonyl group (Scheme 3B in Supplementary material). The band at 1591 cm^{-1} was originated from i.p. stretching vibration of benzene ring (i.e., 8a, according to Wilson's notation [38]) (Scheme 3C in Supplementary material). The intensive peak at 841 cm^{-1} belongs to out-of-plane (o.p.) mode of the last fragmentor 11-γ_{CH} (Scheme 3D in Supplementary material).

The conventional IR-spectra of G30, K4, and systems GK4 and GK4Sm are presented in Fig. 6A. The highest absorption peak in the spectrum in Fig. 6A (1) is at 3224 cm^{-1} and the obtained difference between theoretical and experimental data of $\Delta\nu_{OH}$ of 165 cm^{-1} is explained with the participation of OH group in intermolecular hydrogen bonding. The intensive peaks in 1800–1600 cm^{-1} of $\nu_{C=O}$ are low frequency shifted with $\Delta\nu_{C=O}$ of 23 cm^{-1} and 15 cm^{-1} is also explained with intermolecular interactions. The characteristic maxima for i.p. (8a) and o.p. (11-γ_{CH}) of benzene ring are practically uninfluenced due to the absence of any interaction. The differences between theoretical and experimental values of these and also other maxima for benzene ring are less than 5 cm^{-1}, thus showing an excellent correlation and the good applicability of used theoretical approximation.

As could be seen, the IR-spectral patterns in Fig. 6A (2–4) are practically identical and are similar to IR-spectrum of G30 [Fig. 6A (2)]. The obtained strong overlapped effect of matrix and IR-spectral patterns of investigated compounds resulted in a difficult interpretation of the embedded compound. However, the application of the reducing-difference procedure for non-polarized IR-spectra resulted in reduced IR-curves as shown in Fig. 6A. In spectrum on Fig. 6A (3) the characteristic maxima of K4 in the system GK4 are observed.

However, the detailed explanation of the processes in examined relatively difficult system requires the assignment of IR-bands of all components separately, similar to pure compound K4 stated above. Starting with the reduced IR-spectrum of pure G30 after the subtraction [Fig. 6B (2)] of the bands of H_2O included in the system with the used KBr powder preparing the KBr-pellets [bands at 3400 cm^{-1} and 1627 cm^{-1}; Fig. 6A (2)]. The deconvolution and curve-fitting procedure applied to the spectrum in Fig. 6A (2) resulted in a series of maxima where the bands in 3700–3100 cm^{-1} and about 1660 cm^{-1} correspond to two stretching and banding modes of H_2O molecules intermolecular interacting to two manners, due to only two δ_{H2O} peaks are obtained. These maxima are obtained in the same wave numbers as well in the system GK4 assuming the absence of interactions between matrix and embedded compound K4. Additional confirmation of this assumption follows analysis the IR-absorption peaks of K4 in the spectrum in Fig. 6A (3). As could be seen, all the

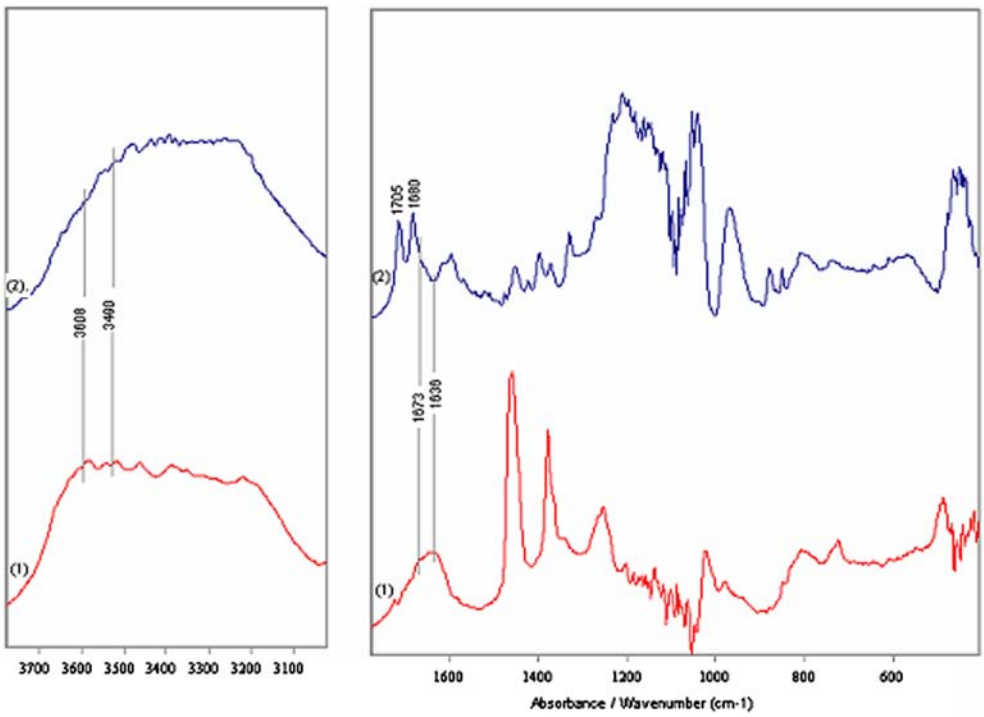

Fig. 7 Reduced IR-spectra of the systems GSm (1) and GK4Sm (2)

characteristic peaks of K4 are practically unchanged and difference less than 1 cm^{-1} is obtained [compare spectra in Fig. 6A (1) and 6A (3)].

The investigation of the system GK4Sm matrix starting with the analysis of Sm^{3+} salt embedded in the matrix (GSm). The reduced IR-spectrum after elimination of the matrix IR-bands is presented in Fig. 7 (1). The curve-fitting procedure arised the maxima at 3613 cm^{-1}, 3503 cm^{-1}, 3367 cm^{-1} and 3231 cm^{-1} corresponding to stretching vibration modes of H_2O as well as the bands at 1673 cm^{-1} and 1636 cm^{-1} corresponding to bending H_2O ones. This means that Sm^{3+} ion is coordinated with two different types of H_2O molecules. As far as the typical coordination numbers of Sm^{3+} are 6 and 8 [37,39–42] it could be assigned that in the octahedral $Sm(III)(H_2O)_6^{3+}$ complex, the equatorial four equivalent molecules are characterized with stretching bands at 3503 cm^{-1} and 3231 cm^{-1} as well as of the 1673 cm^{-1} bending vibration. The axial molecules as weaker coordinated, their characteristic peaks are at 3613 cm^{-1}, 3367 cm^{-1} and 1636 cm^{-1}. The comparison of the reduced IR-spectrum of GSm and this of GK4Sm the following conclusions could be drawn. In the spectrum of the last system the maxima for axial H_2O molecules are disappeared and only for equatorial ones are obtained. As far as K4 is concerned, it does not contain H_2O molecules [see spectrum in Fig. 6A (3)], the discussed bands correspond to solvent included in the inside coordination sphere of Sm(III). The band of $\nu_{C=O}$ in K4 of exocyclic C=O group is low frequency shifted in the system GK4Sm with 8 cm^{-1} and is observed at 1705 cm^{-1}. Similar tendency is obtained for $\nu^{as}{}_{COC}$ and $\nu^{s}{}_{COC}$ at 1100 cm^{-1} and 910 cm^{-1} [Fig. 6A (1)] in K4, where the low frequency shifting is with 9 cm^{-1} and 11 cm^{-1}, respectively [see Fig. 7 (2)]. The band of $\nu_{C=O}$ of ester carbonyl group is practically unaffected and is obtained at 1680 cm^{-1}. The o.p. 11-γ_{CH} maximum is practically uninfluenced, which is typical for other Sm^{3+} complexes [37,39–42]. These data assumed a formation of the Sm(III) complex with K4 in the last system studied with an assumed structure, presented in Scheme 2,3 where the coordination number of metal ion is 8 and the geometry of the chromophor SmO_8 is slightly distorted capped-square-antiprism polyhedron. The data correlated well with the UV- and luminescence result discussed before. Moreover, the lanthanide complexes of types $[LnL_2 \times H_2O]^{3-}$, where Ln = Sm^{3+}, Eu^{3+}, Gd^{3+}, Tb^{3+} and Hp^{3+} have been studied by single crystal X-ray differaction and the data show a coordination number 8 of the metal ions [37,39–42].

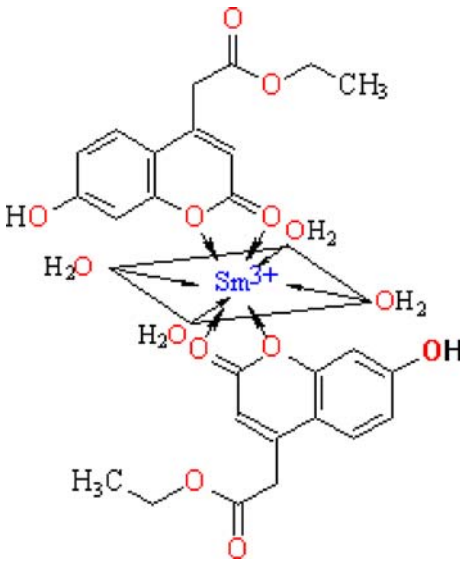

Scheme 2 Chemical diagram of Sm^{3+} complex with K4

Conclusions

Synthesis, NMR, IR-, UV/Vis, and luminescence spectroscopic and theoretical investigations of new monolith

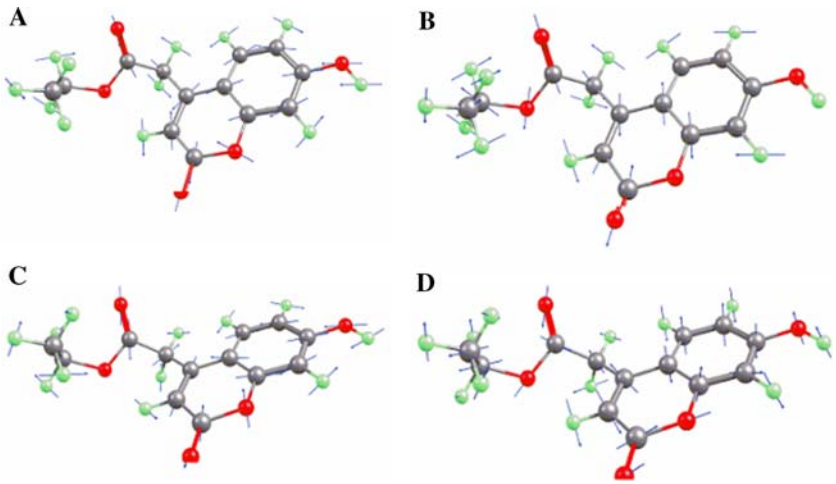

Scheme 3 Transition moments in K4

materials with potential optical application, based on sol-gel technology of incorporated organic molecule [ethyl 2-(7-hydroxy-2-oxo-2H-chromen-4-yl)-acetate] and Sm^{3+} ions are reported. The preparation of large crack-free, transparent SiO_2 xerogels doped with coumarin molecules or co-doped with coumarin molecules and Sm^{3+} ions is possible by using a sol-gel preparation schema based on soft drying conditions at room temperature. Both absorption peak maxima and relative intensities of the coumarin molecules are changed after incorporation of Sm^{3+} ions in the gel network, which gives an indication for complex formation. The structure of the coordination compound is obtained by means of the IR-spectroscopic analysis using the reducing-difference procedure for non-polarized IR-spectra interpretation. Coumarin interacted bidentately through two O-atoms from exocyclic C = O and lactonic groups with metal ion forming the $[Sm(III)L_2 \times (H_2O)_4] \times (NO_3)_3$. The geometry of the SmO_8 chromophor is slightly distorted capped-square-antiprism polyhedron. The IR results suggest that the gel matrix did not interact with doped organic compound.

Acknowledgments G.A. and I.P. thank the Ministry of Education for the Project ''Leading University Research Centre for Nanoscience and Knowledge based Materials''. S.G. was supported by a Project BYX 08/05. B.K. thanks Alexander von Humboldt Foundation for supporting scientific research.

References

1. Levy, D.: Photochromic sol-gel materials. Chem. Mater. **9**, 2666–2670 (1997).
2. Higginbotham, C., Pike, Ch.F., Rice, J.K.: Spectroscopy in sol-gel matrices. J. Chem. Educ. **75**(4), 461–464 (1998).
3. Mauritz, K.A.: http://www.psrc.usm.edu/mauritz/solgel.html. Cited 3 March 2005 (2005).
4. Krihak, M., Murtagh, M.T., Shahriari, M.R.: A spectroscopic study of the effects of various solvents and sol-gel hosts on the chemical and photochemical properties of Thionin and Nile Blue A. J. Sol-gel Sci. Technol. **10**, 153–163 (1997).
5. Shou, H., Ye, J., Yu, Q.: Luminescence properties of benzoic acid-terbium complexes. J. Lumin. **42**, 29 (1988).
6. Curry, R.J., Gillin, W.P.: 1.54 μm electroluminescence from Erbium (III) tris(8-hydroxyquinoline) (ErQ)-based organic light-emitting diodes. Appl. Phys. Lett. **75**(10), 1380–1382 (1999).
7. Steemers, F.J., Verboom, W., Reinhoudt, D.N., van der Tal, E.B., Verhoeven, J.W.: New sensitizer-modified Calix[4]arenas enabling near-UV exitation of complexed luminescent lanthanide ions. J. Am. Chem. Soc. **117**, 9408–9414 (1995).
8. Roh, S.-G., Baek, N.S., Hong, K.-S., Oh, J.B., Kim, H.K.: Synthesis and photophysical properties of luminescent Erbium (III) complexes based on Coumarin derivatives for advanced photonics applications. Mol. Cryst. Liq. Cryst. **425**, 167–172 (2004).
9. Kostova, I.P., Manolov, I.I., Radulova, M.K.: Stability of the complexes of some lanthanides with Coumarin derivatives. I. Cerium(III)-4-methyl-7hydroxycoumarin. Acta Pharm. **54**, 37–47 (2004).
10. Kostova, I.P., Manolov, I.I., Radulova, M.K.: Stability of the complexes of some lanthanides with Coumarin derivatives. II. Neodymium(III)-acenocoumarol. Acta Pharm. **54**, 119–131 (2004).
11. Dann, O., Illing, G.: Über Den Verlauf Der Pechmann-Reaktion. Liebigs Ann. Chem. **605**, 158–167 (1957).
12. Körner, P.: 3-Alkyl- and 3-Aryl-(7-oxo-7*H*-furo3,2-g]chromen-5-yl)alkanoic acids as inhibitors of leukotriene B_4 biosynthesis. Arch. Pharm. Pharm. Med. Chem. **336**, 273–284 (2003).
13. Bredol, M., Gutzov, S.: Effect of germanium codoping on the luminescence of Terbium doped silica xerogels. Opt. Mater. **20**, 233–239 (2002).
14. Gutzov, S., Bredol, M.: Preparation and optical properties of silica xerogels doped with rare earth ions. C. R. Acad. Bulg. Sci. **56**, 37–42 (2002).
15. Bredol, M., Gutzov, S., Jüstel, Th.: Preparation and optical properties of holmium doped silica xerogels. J. Non-Cryst. Solids **321**, 1105–1107 (2003).
16. Gutzov, S., Bredol, M.: J. Mat. Sci. Lett. **41** (2006), doi: 10.1007/s10853-005-2184-4.
17. Myers J.L., Well A.D.: Research Design and Statistical Analysis. Harper Collins, New York, pp. 14–155 (1991).
18. Spiegel M.R.: Theory and Problems of Probability and Statistics. McGraw-Hill, New York, pp. 116–117 (1992).
19. Park, J.W., Ferracane, J.L.: Measuring the residual stress in dental composites using a ring slitting method. Dent. Mater. **21**(9), 882–889 (2005).
20. Ivanova, B.B., Tsalev, D.L., Arnaudov, M.G.: Validation of reducing-difference procedure for the interpretation of non-polarized infrared spectra of n-component solid mixtures. Talanta **69**, 822–828 (2006).
21. Arnaudov, M.G., Dimitriev, Y.: Study on the structural transition in binary tellurite glasses by means of reduced infrared spectra. Phys. Chem. Glasses **42**, 99–102 (2001).
22. Gillette, P.C., Koenig, J.L.: Objective criteria for absorbance subtraction. Appl. Spectrosc. **38**, 334–337 (1984).
23. Friese, M.A., Banerjee, S.: Lignin determination by FT-IR. Appl. Spectrosc. **46**, 246–248 (1992).
24. Banerjee, S., Li, K.: Interpreting multicomponent infrared spectra by derivative minimization. Appl. Spectrosc. **45**, 1047–1049 (1991).
25. DALTON (2005) A molecular electronic structure program, Release 2.0. http://www.kjemi.uio.no/software/dalton/dalton.html. Cited 5 Mar 2005.
26. Zhurko, G.A., Zhurko, D.A.: ChemCraft: Tool for treatment of chemical data, Lite version build 08 (freeware) (2005).
27. Becke, A.D.: Density-functional thermochemistry. III. The role of exact exchange. J. Chem. Phys. **98**, 5648–5652 (1993).
28. Lee, C., Yang, W., Parr, R.G.: Development of the colle-salvetti correlation-energy formula into a functional of the electron density. Phys. Rev. B. **37**, 785–789 (1988).
29. Peng, C., Ayala, Y., Schlegel, H.B., Frisch, M.J.: Using redundant internal coordinates to optimize equilibrium geometries and transition states. J. Comp. Chem. **17**(1), 49–56 (1996).
30. Scott, A.P., Radom, L.J.: Harmonic vibrational frequencies: an evaluation of hartree-fock, Møller-Plesset, quadratic configuration interaction, density functional theory, and semiempirical scale factors. J. Phys. Chem. **100**, 16502–16513 (1996).
31. Hehre W.J., Radom L., Schleyer, P.v.R., Pople J.A.: Ab Initio MO, Theory. Wiley, New York, pp. 9–45 (1986).
32. Foresman, J.B., Head-Gordon, M., Pople, J.A., Frish, M.J.: Toward a systematic molecular orbital theory for excited states. J. Phys. Chem. **96**, 135–146 (1992).
33. Kodaira, C.A., Brito, H.E., Teotonia, E.S., Felinto, M., Malta, O.L., Brito, G.: Photoluminescence behavior of the Sm^{3+} and Tb^{3+} ions doped into the $Gd_2(WO_4)_3$ matrix prepared by the Pechini and Ceramic methods. J. Braz. Chem. Soc. **15**(6), 890–896 (2004).

34. Shionoya, Sh., Yen, W.M.: Phosphor Handbook. CRC Press, Boca Raton, p. 184 (1999).
35. Alonso, M.-T., Brunet, E., Juanes, O., Rodrìguez-Ubis, J.-C.: Synthesis and photochemical properties of new Coumarin-derived ionophores and their alkaline-earth and Lanthanide complexes. J. Photochem. Photobiol. A: Chem. **147**, 113–125 (2002).
36. Brankova, T., Bekiari, V., Lianos, P.: Photoluminescence from sol-gel organic/inorganic hybrid gels obtained through carboxylic acid solvolysis. Chem. Mater. **15**, 1855–1859 (2003).
37. Kang, J.-G., Kang, H.-J., Jung, J.-S., Yun, S.S., Kim, Ch.-H.: Crystal structures and luminescence properties of $[Ln(NTA)_2{\cdot}H_2O]^{3-}$ complexes (Ln = Sm^{3+}, Eu^{3+}, Gd^{3+}, Tb^{3+}, Ho^{3+}, and NTA = Nitrilotriacetate). Bull. Korean Chem. Soc. **25**(6), 852–858 (2004).
38. Varsanyi, G.: Vibrational Spectra of Benzene Derivatives. Academy Press, Budapest, pp. 1–413 (1969).
39. Chung, D.Y., Lee, E.H., Kimura, T.: Laser-induced luminescence study of Samarium(III) Thiodiglycolate complexes. Bull. Korean Chem. Soc. **24**(9), 1396–1398 (2003).
40. Zhang, J.-J., Ren, N., Wang, Y.-X., Xu, S.-L., Wang, R.-F., Wang, S.-P.: Synthesis, crystal structure and thermal decomposition mechanism of a samarium o-Chlorobenzoate complex with 1,10-Phenanthroline. J. Braz. Chem. Soc. **17**(7), 1355–1359 (2006).
41. Ferenc, W., Walków-Dziewulskaj, A.: Complexes of light lanthanides with 2,4-dimethoxybenzoic acid. Serb. Chem. Soc. **65**(1), 27–35 (2000).
42. Wang, R., Liu, H., Carducci, M.D., Jin, T., Zheng, Ch., Zheng, Z.: Lanthanide coordination with r-amino acids under near physiological pH conditions: Polymetallic complexes containing the cubane-Like $[Ln4(\mu_3\text{-}OH)_4]^{8+}$. Cluster Core Inorg. Chem. **40**, 2743–2750 (2001).